Vol 18 No 4, April 2009
1674-1056/2009/18(04)/1691-09

Chinese Physics B

© 2009 Chin. Phys. Soc.
and IOP Publishing Ltd

The effect of anisotropic surface tension on the morphological stability of planar interface during directional solidification*

Chen Ming-Wen(陈明文)[a], Lan Man(兰 曼)[a], Yuan Lin(袁 琳)[a],
Wang Yu-Yan(王玉燕)[a], Wang Zi-Dong(王自东)[b]†, and Xu Jian-Jun(徐鉴君)[b][c][d]

[a] *School of Applied Sciences, University of Science and Technology Beijing, Beijing* 100083, *China*
[b] *School of Materials Science and Engineering, University of Science and Technology Beijing, Beijing* 100083, *China*
[c] *School of Mathematical Sciences, Nankai University, Tianjin* 300071, *China*
[d] *Department of Mathematics and Statistics, McGill University, Montreal H3A 2K6, Canada*

(Received 30 July 2008; revised manuscript received 28 August 2008)

This paper considers the effect of the anisotropic surface tension on the morphological stability of the planar interface during directional solidification. When the expression exhibiting the four-fold symmetry is included, the modified absolute stability criterion is obtained by employing the multi-variable expansion method. The linear stability analysis reveals that for the given temperature gradient, as the anisotropic surface tension parameter increases, the stability zone tends to decrease.

Keywords: directional solidification, planar interface, anisotropic surface tension, morphological stability

PACC: 8130F, 8110F, 6470D

1. Introduction

Directional solidification techniques have been widely applied in manufacturing high-quality single crystals and other metal materials. The small-scale details of the solidification for the undercooled melt, including the anisotropic surface energy and anisotropic interface kinetics, can significantly affect the morphology of solid-liquid interface and the microstructure of the final materials. The examination of kinetic effects made by Wilcox[1] revealed that crystals growing in a faceted manner is favoured by anisotropic growth kinetics. Coriell and Sekerka[2] considered the anisotropic departure from local equilibrium at the solid-liquid interface and modified the theory of the morphological stability of a planar interface. Their results showed that anisotropic interface kinetics leads to the additional effect that sinusoidal perturbations are translated parallel to the unperturbed interface as they change in amplitude. The peaks of such sinusoidal perturbations grow at an angle to the normal of the unperturbed interface. Young *et al*[3] made the long-wave instability analysis of a planar interface and showed that the anisotropic surface energy causes the cells to grow at an angle to the normal of the planar front. This transition to a cellular morphology is shown to be a subcritical instability. Vigdergauz and Givoli[4] developed a perturbation solution technique that is valid for cubic crystals with weak anisotropy. Their numerical results confirmed that a GaAs boule grows as a function of the anisotropy parameter. Satoa and Uwahaa[5] studied the effect of anisotropy in step kinetics on the wandering instability of an isolated step and found that near the threshold of the instability, the anisotropy effect becomes strong while that of the step stiffness becomes weak. Golovin and Davis[6] carried out the morphological stability analysis of rapid solidification in a hypercooled melt and revealed that due to anisotropy the threshold of morphological instability depends on the direction of the crystal growth and generates travelling waves propagating on the solidification front in a

*Project supported by the National Basic Research Program of China (the Project 973) (Grant No 2006CB605205) and the National Natural Science Foundation of China (Grant No 10672019).
†Corresponding author. E-mail: wangzdg@263.net

preferred direction determined by the anisotropy coefficients. Coriell and McFadden[7] analysed the effect of anisotropic interface kinetics on the onset of instability during growth from a supersaturated solution. The kinetic anisotropy arises from a model of step motion in which the morphological instability corresponds to step bunching. Kinetic anisotropy causes travelling waves along the crystal-solution interface and an enhancement of morphological stability. By including the effects of surface energy with cubic anisotropy on nanoscale pattern formation during the electropolishing of aluminium, Guo and Johnson[8] found that increasing the surface energy can extend the stability range of hexagons. Norris and Davis *et al*[9,10] investigated the directional solidification of a dilute binary alloy having a large anisotropy of surface energy, (i.e., orientations with negative surface stiffness), the linear stability analysis revealed that the planar state is thermodynamically prohibited, leading to a family of faceted interface profiles, confirms a small optimal wavelength and an associated facet-velocity law. Lü *et al*[11] made a numerical simulation for 4H-SiC MESFET anisotropy and showed obvious effects of the anisotropy for 4H-SiC, and pointed out that the anisotropy for 4H-SiC should be involved in the device design to acquire better performances. Yan *et al*[12] found in the analysis of the magnetization curves for Gd_2Fe_{17} and $Gd_2Fe_{17}H_3$ that if the Gd-Fe exchange interaction has been taken as isotropic, the fitted values of magneto-crystalline anisotropy of the Fe sublattices would become unreasonably different from those of the corresponding Y or Lu compounds, and the large difference is caused by the neglect of the anisotropy of the Gd-Fe exchange interaction. Analytically, after the systematical analysis, Xu[13,14] concluded that the any perturbed states in the directional solidification from the pure melt are either purely growing or purely decaying and have a unique neutrally stable state.

During directional solidification the surface energy is actually anisotropic. There exist boundary layers in the vicinity of the interface in solidification, which separate the whole physical region into several sub-regions that may differ by several orders of magnitude in scales. By using the multi-variable expansion method that is developed by Xu,[13−20] we study the effect of the anisotropic surface energy on the morphological stability of the planar front in directional solidification.

2. Formation of the system

Consider the directional solidification of an undercooled alloy melt, as shown in Fig.1. A liquid-solid interface is moving upward with a pulling velocity V in the reference in which the solid phase is at rest. It is assumed that the concentration at the far field is $\bar{C}_\infty$. At the edge of the liquid phase zone, $\bar{y} = \bar{L}_1$,

$$\bar{T}_L = \bar{T}_H.$$

At the edge of the solid phase zone, $\bar{y} = -\bar{L}_2$,

$$\bar{T}_L = \bar{T}_C.$$

The distance between the edges of two zones is set to be $\bar{L}$, $\bar{L} = \bar{L}_1 + \bar{L}_2$. The temperatures in the liquid and solid phases are denoted by $\bar{T}_L$ and $\bar{T}_S$, respectively. The concentrations in the liquid and solid phases are denoted by $\bar{C}_L$ and $\bar{C}_S$, respectively. Thus it holds $\bar{T}_C < \bar{T}_S \leq \bar{T}_L < \bar{T}_H$. The liquid-solid interface is expressed as $\bar{y} = \bar{h}(\bar{x}, \bar{t})$. The anisotropic surface energy is described by the four-fold symmetric function $\gamma(\theta) = \gamma_0(1 + \alpha_4 \cos 4\theta)$, where γ_0 is the dimensional isotropy which gives the average magnitude of $\gamma(\theta)$, θ is the angle between the surface normal and the y axis and α_4 is the anisotropy parameter. We also assume that the densities ρ_L and ρ_S in the liquid and solid phases are equal and the specific heats in the liquid phase and solid phase are equal, and the buoyancy effects are neglected.

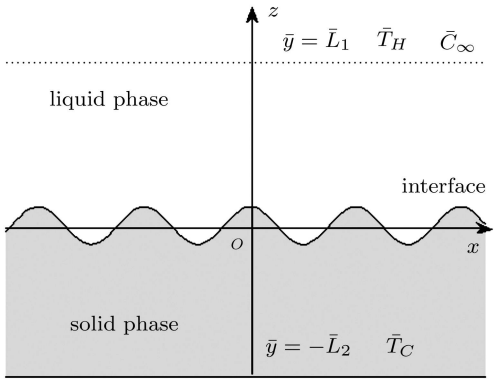


Fig.1. A sketch of two-dimensional directional solidification system.

The solidification system is governed by the temperature and concentration equations, subject to the boundary conditions: the thermodynamic equilibrium and Gibbs–Thomson conditions, the energy conservation condition, and far field conditions. We choose the velocity of the interface V as the scale for the velocity, the solute diffusion length ℓ_D ($\ell_D = \kappa_D/V$) as the

length scale, where κ_D is the thermal diffusivity in the liquid phase, κ_D/V^2 as the time scale, and $\Delta H/(c_p\rho_L)$ as the temperature scale, where ΔH is the latent heat per unit volume of the solid phase and c_p the specific heat. We introduce the following dimensionless quantities:

$$T_L = \frac{\bar{T}_L - \bar{T}_M}{\Delta H/(c_p\rho_L)}, \quad T_S = \frac{\bar{T}_S - \bar{T}_M}{\Delta H/(c_p\rho_L)},$$
$$C_L = \frac{\bar{C}_L}{\bar{C}_\infty}, \qquad C_S = \frac{\bar{C}_S}{\bar{C}_\infty}, \tag{1}$$

where $\bar{T}_M$ is the equilibrium temperature at the flat interface. In the moving frame (x, y, z) with its x axis attached to the mean planar location of the interface that moves toward the y direction, the dimensionless spatial and time coordinates are denoted by

$$(x, y, t) = \left(\frac{\bar{x}}{\ell_D}, \frac{\bar{y} - V\bar{t}}{\ell_D}, \frac{V\bar{t}}{\ell_D}\right), \tag{2}$$

the curved interface in the moving frame is expressed as $y = h(x, t)$. Thus the solidification system is described by the following equations and boundary conditions with the two-dimensional form:

$$\lambda\left(\frac{\partial T_L}{\partial t} - \frac{\partial T_L}{\partial y}\right) = \nabla^2 T_L \quad (h(x,t) < y < \infty), \tag{3}$$

$$\lambda\alpha_T\left(\frac{\partial T_S}{\partial t} - \frac{\partial T_S}{\partial y}\right) = \nabla^2 T_S \quad (-\infty < y < h(x,t)), \tag{4}$$

$$\frac{\partial C_L}{\partial t} - \frac{\partial C_L}{\partial y} = \nabla^2 C_L \quad (h(x,t) < y < \infty), \tag{5}$$

where $\lambda = \kappa_D/\kappa_T$, $\alpha_T = \kappa_T/\kappa_S$, κ_S is the thermal diffusivity in the solid phase. In the present paper, the concentration in the solid phase is treated to be constant.

The interface conditions: at the interface $y = h(x, t)$,

$$T_L = T_S, \tag{6}$$

$$T_S = 2\Gamma\left(1 - 15\alpha_4\cos 4\theta\right)\frac{h_{xx}}{(1+h_x^2)^{3/2}} - S^{-1}M\frac{1+h_t}{(1+h_x^2)^{1/2}} - M_C C_L, \tag{7}$$

$$\lambda\frac{1+h_t}{(1+h_x^2)^{1/2}} + \left(\frac{\partial}{\partial y} - h_x\frac{\partial}{\partial x}\right)\left(\hat{k}T_S - T_L\right) = 0, \tag{8}$$

$$(1-k)C_L\frac{1+h_t}{(1+h_x^2)^{1/2}} = h_x\frac{\partial C_L}{\partial x} - \frac{\partial C_L}{\partial y}, \tag{9}$$

where $\hat{k} = k_S/k_T$, k_T and k_S are the thermal conduction coefficients in the liquid and the solid phases, respectively. $\Gamma = \ell_c/\ell_D$, $\ell_c = \gamma_0 c_p\rho_L T_M/(\Delta H)^2$ is the capillary length, $S = \Delta H/(c_p\rho_L T_M)$, $M = V/(\mu T_M)$, μ is the interfacial kinetic coefficient, $M_C = \dfrac{-m\bar{C}_\infty}{\Delta H/(c_p\rho_L)}$, m is the slope of the liquidus in the phase diagram.

The far field condition: as $y \to +\infty$,

$$T_L \to T_\infty, \quad C_L \to 1, \tag{10}$$

where

$$T_\infty = \frac{\bar{T}_\infty - \bar{T}_M}{\Delta H/(c_p\rho_L)}.$$

And the initial condition at the time $t = 0$. Note that the initial condition is not necessary for the stability analysis.

3. Linear stability analysis

The basic state solution with the planar interface is obtained by setting $\dfrac{\partial}{\partial t} = 0$ and $\dfrac{\partial}{\partial x} = 0$ from Eqs.(3)–(10):

$$T_{LB}(y) = A_1 + A_2 e^{-\lambda y}, \tag{11}$$
$$T_{SB}(y) = A_{S1} + A_{S2} e^{\lambda y}, \tag{12}$$
$$C_{LB}(y) = 1 + \frac{1-k}{k}e^{-y}, \tag{13}$$

where

$$A_1 = \frac{T_H + \dfrac{M_C}{k}e^{-\lambda L_1}}{1 - e^{-\lambda L_1}}, \quad A_2 = \frac{-\left(T_H + \dfrac{M_C}{k}\right)}{1 - e^{-\lambda L_1}},$$
$$A_{S1} = \frac{T_C + \dfrac{M_C}{k}e^{-\lambda L_2}}{1 - e^{-\lambda L_2}}, \quad A_{S2} = \frac{-\left(T_C + \dfrac{M_C}{k}\right)}{1 - e^{-\lambda L_2}}.$$

It is easy to determine the location of the interface. For any given L, $L = L_1 + L_2$, we can find L_1 and L_2:

$$L_1 = \frac{L}{R}, \quad L_2 = \left(1 - \frac{1}{R}\right)L, \quad \text{and}$$
$$R = \frac{T_H - T_C}{T_H + \dfrac{M_c}{k} + S^{-1}M}.$$

To carry out the morphological stability analysis, we express the temperature and concentration fields

and the interface as the superimposition of the basic state and the correction terms

$$T_L(x,y,t) = T_{LB}(x,y,t) + \tilde{T}_L(x,y,t), \quad (14)$$

$$T_S(x,y,t) = T_{SB}(x,y,t) + \tilde{T}_S(x,y,t), \quad (15)$$

$$C_L(x,y,t) = C_{LB}(y) + \tilde{C}_L(x,y,t), \quad (16)$$

$$h(x,t) = h_B + \widetilde{h}(x,t), \quad (17)$$

where $h_B(x,t) = 0$ is the mean planar location of the interface, and $\tilde{T}_L, \tilde{T}_S, \tilde{C}_L, \tilde{h}$ are small perturbations around the steady state. With Eqs.(14)–(17), the linearized equations and boundary conditions are transformed into:

$$\lambda\left(\frac{\partial \tilde{T}_L}{\partial t} - \frac{\partial \tilde{T}_L}{\partial y}\right) = \nabla^2 \tilde{T}_L, \quad (18)$$

$$\lambda\alpha_T\left(\frac{\partial \tilde{T}_S}{\partial t} - \frac{\partial \tilde{T}_S}{\partial y}\right) = \nabla^2 \tilde{T}_S, \quad (19)$$

$$\frac{\partial \tilde{C}_L}{\partial t} - \frac{\partial \tilde{C}_L}{\partial y} = \nabla^2 \tilde{C}_L, \quad (20)$$

which are subjected to the interface conditions:

$$\tilde{T}_L = \tilde{T}_S - \Delta G_1 \tilde{h}, \quad (21)$$

$$\tilde{T}_S = \Gamma(1-15\alpha_4)\frac{\partial^2 \tilde{h}}{\partial x^2} - G_{S1}\tilde{h} - M_C\tilde{C}_L + \frac{1-k}{k}M_C\tilde{h} - S^{-1}M\frac{\partial \tilde{h}}{\partial t}, \quad (22)$$

$$\lambda\frac{\partial \widetilde{h}}{\partial t} = -\frac{\partial}{\partial y}(\tilde{T}_L - \hat{k}\tilde{T}_S) - \Delta G_2\widetilde{h}, \quad (23)$$

$$\frac{\partial \tilde{C}_L}{\partial y} + \frac{1-k}{k}\frac{\partial \tilde{h}}{\partial t} + (1-k)(\tilde{C}_L + \tilde{h}) = 0, \quad (24)$$

where

$$\Delta G_1 = G_{L1} - G_{S1},$$
$$\Delta G_2 = \frac{\partial^2 T_{LB}(0)}{\partial y^2} - \hat{k}\frac{\partial^2 T_{SB}(0)}{\partial y^2},$$
$$G_{L1} = \frac{\partial T_{LB}(0)}{\partial y}, \quad G_{S1} = \frac{\partial T_{SB}(0)}{\partial y},$$
$$G_{C1} = \frac{\partial C_{SB}(0)}{\partial y},$$

and the far field conditions: as $y \to +\infty$,

$$\tilde{T}_L \to 0, \quad \tilde{C}_L \to 0, \quad (25)$$

and as $y \to -\infty$,

$$\tilde{T}_S \to 0. \quad (26)$$

For the typical metals, the surface energy parameter Γ is in the range of $\Gamma \approx 10^{-2} \sim 10^{-5}$. As shown by Xu,[13,14] the parameter Γ is treated as the interfacial stability parameter, that is $\Gamma = \varepsilon^2$, $\varepsilon \ll 1$. The parameter ε plays a dominant role in the linear stability analysis. When the kinetic undercooling is small, it is assumed that $M = \varepsilon\hat{M}$ and $\hat{M} = O(1)$. It is well known that the macroscopic transport processes mainly occur near the liquid-solid interface where the temperature and concentration are dramatically changed. The argument gives us a hint that there is a boundary layer near the liquid-solid interface. Since a small parameter ε appears in front of the second derivative $\dfrac{\partial^2 \tilde{h}}{\partial x^2}$ in Eq.(22), balancing the magnitude at the two sides leads to the structure of multiple length scales, then we introduce a set of fast variables

$$t_+ = \frac{\sigma(\varepsilon)}{\varepsilon}t, \quad x_+ = \frac{k(\varepsilon)}{\varepsilon}x,$$
$$y_+ = \frac{g(\varepsilon)}{\varepsilon}y \ \text{(for temperature in the liquid phase)};$$
$$y_+ = \frac{g_S(\varepsilon)}{\varepsilon}y \ \text{(for temperature in the liquid phase)};$$
$$y_+ = \frac{q(\varepsilon)}{\varepsilon}y \ \text{(for concentration in the liquid phase)}, \quad (27)$$

where $\sigma(\varepsilon)$, $k(\varepsilon)$, $g(\varepsilon)$, $g_S(\varepsilon)$ and $q(\varepsilon)$ are to be determined. It is further assumed that they have the following asymptotic expansions,

$$\sigma(\varepsilon) = \sigma_0 + \varepsilon\sigma_1 + \cdots, \quad k(\varepsilon) = k_0 + \varepsilon k_1 + \cdots,$$
$$g(\varepsilon) = k_0 + \varepsilon g_1 + \cdots, \quad g_S(\varepsilon) = k_0 + \varepsilon g_{S1} + \cdots,$$
$$q(\varepsilon) = k_0 + \varepsilon q_1 + \cdots, \quad (28)$$

in which σ_0, σ_1, k_0, k_1, g_1, g_{S1} and q_1, ... are constants to be determined. The fast variables x_+, y_+, t_+ and the slow variables x, y, t are formally treated as the independent variables. With the new variables, equations (18)–(24) are transformed into

$$k^2\frac{\partial^2 \tilde{T}_L}{\partial x_+^2} + g^2\frac{\partial^2 \tilde{T}_L}{\partial y_+^2} = \varepsilon\left(\lambda\sigma\frac{\partial \tilde{T}_L}{\partial t_+} - \lambda g\frac{\partial \tilde{T}_L}{\partial y_+} - 2k\frac{\partial^2 \tilde{T}_L}{\partial x \partial x_+} - 2g\frac{\partial^2 \tilde{T}_L}{\partial y \partial y_+}\right) - \varepsilon^2\left(\nabla^2\tilde{T}_L + \lambda\frac{\partial \tilde{T}_L}{\partial y} - \lambda\frac{\partial \tilde{T}_L}{\partial t}\right), \quad (29)$$

$$k^2\frac{\partial^2\tilde{T}_S}{\partial x_+^2}+g_S^2\frac{\partial^2\tilde{T}_S}{\partial y_+^2}=\varepsilon\left(\lambda\alpha_T\sigma\frac{\partial\tilde{T}_S}{\partial t_+}-\lambda\alpha_T g_S\frac{\partial\tilde{T}_S}{\partial y_+}-2k\frac{\partial^2\tilde{T}_S}{\partial x\partial x_+}-2g_S\frac{\partial^2\tilde{T}_S}{\partial y\partial y_+}\right)$$
$$-\varepsilon^2\left(\nabla^2\tilde{T}_S+\lambda\alpha_T\frac{\partial\tilde{T}_S}{\partial y}-\lambda\alpha_T\frac{\partial\tilde{T}_S}{\partial t}\right), \tag{30}$$

$$k^2\frac{\partial^2\tilde{C}_L}{\partial x_+^2}+q^2\frac{\partial^2\tilde{C}_L}{\partial y_+^2}=\varepsilon\left(\sigma\frac{\partial\tilde{C}_L}{\partial t_+}-q\frac{\partial\tilde{C}_L}{\partial y_+}-2k\frac{\partial^2\tilde{C}_L}{\partial x\partial x_+}-2q\frac{\partial^2\tilde{C}_L}{\partial y\partial y_+}\right)-\varepsilon^2\left(\nabla^2\tilde{C}_L+\frac{\partial\tilde{C}_L}{\partial y}-\frac{\partial\tilde{C}_L}{\partial t}\right). \tag{31}$$

The interface conditions are

$$\tilde{T}_L=\tilde{T}_S-\Delta G_1\widetilde{h}, \tag{32}$$

$$\tilde{T}_S=\left[k^2\frac{\partial^2\widetilde{h}}{\partial x_+^2}+2\varepsilon k\frac{\partial^2\widetilde{h}}{\partial x\partial x_+}+\varepsilon^2\frac{\partial^2\widetilde{h}}{\partial x^2}\right](1-15\alpha_4)-G_{S1}\widetilde{h}-S^{-1}\hat{M}\left(\sigma\frac{\partial\widetilde{h}}{\partial t_+}+\varepsilon\frac{\partial\widetilde{h}}{\partial t}\right)$$
$$-M_C\tilde{C}_L+\frac{1-k}{k}M_C\tilde{h}, \tag{33}$$

$$g\frac{\partial\tilde{T}_L}{\partial y_+}-\hat{k}g_S\frac{\partial\tilde{T}_S}{\partial y_+}+\varepsilon\frac{\partial}{\partial y}(\tilde{T}_L-\hat{k}\tilde{T}_S)+\lambda\sigma\frac{\partial\widetilde{h}}{\partial t_+}+\varepsilon\lambda\frac{\partial\widetilde{h}}{\partial t}+\varepsilon\Delta G_2\widetilde{h}=0, \tag{34}$$

$$q\frac{\partial\tilde{C}_L}{\partial y_+}+\varepsilon\frac{\partial\tilde{C}_L}{\partial y}+\frac{1-k}{k}\left(\sigma\frac{\partial\tilde{h}}{\partial t_+}+\varepsilon\frac{\partial\tilde{h}}{\partial t}\right)+\varepsilon(1-k)(\tilde{C}_L+\tilde{h})=0. \tag{35}$$

We further seek the following asymptotic expansion of correction terms in Eqs.(14)–(17):

$$\tilde{T}_L\sim\mathrm{e}^{t_+}\left(\tilde{T}_{L0}(x,y,x_+,y_+)+\varepsilon\tilde{T}_{L1}(x,y,x_+,y_+)+\cdots\right), \tag{36}$$

$$\tilde{T}_S\sim\mathrm{e}^{t_+}\left(\tilde{T}_{S0}(x,y,x_+,y_+)+\varepsilon\tilde{T}_{S1}(x,y,x_+,y_+)+\cdots\right), \tag{37}$$

$$\tilde{C}_L\sim\mathrm{e}^{t_+}\left(\tilde{C}_0(x,y,x_+,y_+)+\varepsilon\tilde{C}_1(x,y,x_+,y_+)+\cdots\right), \tag{38}$$

$$\tilde{h}\sim\mathrm{e}^{t_+}\left(\tilde{h}_0(x,y,x_+,y_+)+\varepsilon\tilde{h}_1(x,y,x_+,y_+)+\cdots\right). \tag{39}$$

Substituting Eqs.(36)–(39) into (29)–(35) with (25) and (26), one can successively derive each order of approximation. The leading order equations and boundary conditions are as follows:

$$k_0^2\left(\frac{\partial^2\tilde{T}_{L0}}{\partial x_+^2}+\frac{\partial^2\tilde{T}_{L0}}{\partial y_+^2}\right)=0, \tag{40}$$

$$k_0^2\left(\frac{\partial^2\tilde{T}_{S0}}{\partial x_+^2}+\frac{\partial^2\tilde{T}_{S0}}{\partial y_+^2}\right)=0, \tag{41}$$

$$k_0^2\left(\frac{\partial^2\tilde{C}_0}{\partial x_+^2}+\frac{\partial^2\tilde{C}_0}{\partial y_+^2}\right)=0. \tag{42}$$

The interface conditions are

$$\tilde{T}_{L0}=\tilde{T}_{S0}-\Delta G_1\widetilde{h}_0, \tag{43}$$

$$\tilde{T}_{S0}=(1-15\alpha_4)k_0^2\frac{\partial^2\widetilde{h}_0}{\partial x_+^2}-G_{S1}\widetilde{h}_0-S^{-1}\hat{M}\sigma_0\widetilde{h}_0$$
$$-M_C\tilde{C}_0+\frac{1-k}{k}M_C\tilde{h}_0, \tag{44}$$

$$k_0\frac{\partial}{\partial y_+}(\tilde{T}_{L0}-\hat{k}\tilde{T}_{S0})+\lambda\sigma_0\tilde{h}_0=0, \tag{45}$$

$$k_0\frac{\partial\tilde{C}_0}{\partial y_+}+\frac{1-k}{k}\sigma_0\tilde{h}_0=0. \tag{46}$$

and the far field conditions are

$$\text{as}\quad y_+\to+\infty,\ \tilde{T}_{L0}\to0,\quad \tilde{C}_0\to0, \tag{47}$$

and

$$\text{as } y_+\to+\infty,\ \tilde{T}_{S0}\to0. \tag{48}$$

The equations (40)–(42) with the vanishing conditions (47) and (48) allow the following normal mode solutions:

$$\tilde{T}_{L0} = A_{L0}(x,y)\mathrm{e}^{\mathrm{i}x_+ - y_+}, \quad \tilde{T}_{S0} = A_{S0}(x,y)\mathrm{e}^{\mathrm{i}x_+ + y_+},$$
$$\tilde{C}_0 = B_0(x,y)\mathrm{e}^{\mathrm{i}x_+ - y_+}, \quad \tilde{h}_0 = D_0(x)\mathrm{e}^{\mathrm{i}x_+}. \tag{49}$$

Then the interface conditions (43)–(46) become

$$A_{L0}(x,0) - A_{S0}(x,0) + \Delta G_1 D_0(x) = 0, \tag{50}$$
$$A_{S0}(x,0) + M_C B_0 + I_1 D_0(x) = 0, \tag{51}$$
$$-k_0 A_{L0}(x,0) - k_0\hat{k}A_{S0}(x,0) + \lambda\sigma_0 D_0(x) = 0, \tag{52}$$
$$-k_0 B_0(x,0) + \frac{1-k}{k}\sigma_0 D_0(x) = 0, \tag{53}$$

where

$$I_1 = k_0^2(1-15\alpha_4) + G_{S1} + \sigma_0 S^{-1}\hat{M} - \frac{1-k}{k}M_C.$$

For the homogeneous equations with constant coefficients, the amplitude functions A_{L0}, A_{S0}, B_0, D_0 hold for the arbitrary real number x, thus they must be constants. For the nontrivial solution, we obtain the dispersion relation

$$\sigma_0 = \frac{-k_0(1+\hat{k})}{\lambda + k_0(1+\hat{k})S^{-1}\hat{M} + (1+\hat{k})\frac{1-k}{k}M_C} \times \left((1-15\alpha_4)k_0^2 + G - \frac{1-k}{k}M_C\right), \tag{54}$$

where

$$G = \frac{G_{L1} + \hat{k}G_{S1}}{1+\hat{k}}. \tag{55}$$

Specially, if k_L and k_S are equal, or $\hat{k} = 1$, then

$$\frac{G_{1L} + G_{S1}}{2} \geq \frac{1-k}{k}M_C. \tag{56}$$

This is the well-known constitutional undercooling criterion.[13,14,21]

Given an eigenvalue σ_0, the wave numbers k_0 in Eq.(54) are determined, and k_0 must be positive real numbers. Or else, if the wave number k_0 has an imaginary part, the perturbation will tend to infinity either as $x_+ \to +\infty$, or as $x_+ \to -\infty$. And if the wave number k_0 is a negative number, the $O(1)$ order perturbation for the temperature field, $\tilde{T}_{L0}$, $\hat{C}_0$ will tend to infinity as $y_+ \to +\infty$. Therefore, the eigenvalue σ_0 must be real.

It can be seen from Eq.(54) that the anisotropy of the surface tension is always a destabilizing agent, kinetic parameter M makes the denominator decrease, then it is always a stable factor.

Proceeding to $O(\varepsilon)$ order approximation, one derives that

$$k_0^2\left(\frac{\partial^2\tilde{T}_{L1}}{\partial x_+^2} + \frac{\partial^2\tilde{T}_{L1}}{\partial y_+^2}\right) = a_0\mathrm{e}^{\mathrm{i}x_+ - y_+}, \tag{57}$$
$$k_0^2\left(\frac{\partial^2\tilde{T}_{S1}}{\partial x_+^2} + \frac{\partial^2\tilde{T}_{S1}}{\partial y_+^2}\right) = b_0\mathrm{e}^{\mathrm{i}x_+ - y_+}, \tag{58}$$
$$k_0^2\left(\frac{\partial^2\tilde{C}_1}{\partial x_+^2} + \frac{\partial^2\tilde{C}_1}{\partial y_+^2}\right) = c_0\mathrm{e}^{\mathrm{i}x_+ - y_+}, \tag{59}$$

where

$$a_0 = I_0 A_0 + 2k_0\frac{\partial A_0}{\partial y},$$
$$b_0 = I_{S0}A_{S0}(x,y) - 2k_0\frac{\partial A_{S0}(x,y)}{\partial y},$$
$$c_0 = I_{C0}B_0 + 2k_0\frac{\partial B_0(x,y)}{\partial y},$$

in which,

$$I_0 = \lambda\sigma_0 + \lambda k_0 + 2k_0k_1 - 2k_0g_1,$$
$$I_{S0} = \lambda\alpha_T\sigma_0 - \lambda\alpha_T k_0 + 2k_0k_1 - 2k_0g_{S1},$$
$$I_{C0} = \sigma_0 + k_0 + 2k_0k_1 - 2k_0q_1.$$

The interface conditions are

$$\tilde{T}_{L1} = \tilde{T}_{S1} - \Delta G_1\tilde{h}_1, \tag{60}$$

$$\tilde{T}_{S1} - (1-15\alpha_4)k_0^2\frac{\partial^2\tilde{h}_1}{\partial x_+^2} + M_C\tilde{C}_1 = 2(1-15\alpha_4)k_0k_1\frac{\partial^2\tilde{h}_0}{\partial x_+^2} + \left(\frac{1-k}{k}M_C - G_{1S}\right)\tilde{h}_0 - S^{-1}\hat{M}\sigma_0\tilde{h}_1 - S^{-1}\hat{M}\sigma_1\tilde{h}_0, \tag{61}$$

$$k_0\frac{\partial\tilde{T}_{L1}}{\partial y_+} - \hat{k}k_0\frac{\partial\tilde{T}_{S1}}{\partial y_+} + \lambda\sigma_0\tilde{h}_1 = g_{S1}\frac{\partial\tilde{T}_{S0}}{\partial y_+} - \hat{k}g_1\frac{\partial\tilde{T}_{L0}}{\partial y_+} - \lambda\sigma_1\frac{\partial\tilde{h}_0}{\partial t_+} - \frac{\partial}{\partial y}(\tilde{T}_{L0} - \tilde{T}_{S0}) - \Delta G_2\tilde{h}_0, \tag{62}$$

$$k_0\frac{\partial\tilde{C}_1}{\partial y_+} + \frac{1-k}{k}\sigma_0\frac{\partial\tilde{h}_1}{\partial t_+} = -q_1\frac{\partial\tilde{C}_0}{\partial y_+} - \frac{\partial\tilde{C}_0}{\partial y} - \frac{1-k}{k}\sigma_1\tilde{h}_0 - (1-k)(\tilde{C}_0 + \tilde{h}_0). \tag{63}$$

The far field conditions are

$$\text{as} \quad y_+ \to +\infty,\ \tilde{T}_{L1} \to 0, \quad \tilde{C}_1 \to 0, \tag{64}$$

and

$$\text{as} \quad y_+ \to +\infty, \quad \tilde{T}_{S1} \to 0. \tag{65}$$

To avoid the secular terms in solving Eqs.(57)–(59), we set $a_0 = 0$, $b_0 = 0$, $c_0 = 0$, and without losing generality, $A'_{L0}(y) = A'_{S0}(y) = B'_0(y) = 0$, then

$$g_1 - k_1 = \frac{\lambda}{2}\left(1 + \frac{\sigma_0}{k_0}\right), \quad q_1 - k_1 = \frac{1}{2}\left(1 + \frac{\sigma_0}{k_0}\right),$$
$$g_{S1} = g_1 - \frac{\lambda}{2}(1 + \alpha_T) - \frac{\lambda}{2}(1 - \alpha_T)\frac{\sigma_0}{k_0}. \tag{66}$$

Thus we can seek the normal mode solution for Eqs.(57)–(59) with the vanishing conditions (64) and (65):

$$\tilde{T}_{L1} = A_{L1}(x,y)\mathrm{e}^{\mathrm{i}x_+ - y_+}, \quad \tilde{T}_{S1} = A_{S1}(x,y)\mathrm{e}^{\mathrm{i}x_+ + y_+},$$
$$\tilde{C}_{L1} = B_1(x,y)\mathrm{e}^{\mathrm{i}x_+ - y_+}, \quad \tilde{h}_1 = D_1(x)\mathrm{e}^{\mathrm{i}x_+}. \tag{67}$$

The interface conditions (60)–(63) become

$$A_{L1}(x,0) = A_{S1}(x,0) - \Delta G_1 D_1(x), \tag{68}$$

$$A_{S1}(x,0) + M_C B_1(x,0) + I_1 D_1(x) = I_2 D_0, \tag{69}$$

$$-k_0 A_{L1}(x,0) - k_0\hat{k}A_{S1}(x,0) + \lambda\sigma_0 D_1(x) = I_3 D_0, \tag{70}$$

$$-k_0 B_1(x,0) + \frac{1-k}{k}\sigma_0 D_1(x) = I_4 D_0, \tag{71}$$

where

$$\begin{aligned} I_2 &= -2k_0k_1(1 - 15\alpha_4) - S^{-1}\hat{M}\sigma_1 \\ &\quad + \frac{1-k}{k}M_C - G_{S1}, \\ I_3 &= -\lambda\sigma_1 - \Delta G_2 + \frac{g_{S1}}{1+\hat{k}}\left(\frac{\sigma_0}{k_0} - \Delta G_1\right) \\ &\quad + \hat{k}g_1\left(\lambda\frac{\sigma_0}{k_0} + \hat{k}\Delta G_1\right) + (1+\alpha_4)\lambda S k_0^2, \\ I_4 &= q_1\frac{1-k}{k}\frac{\sigma_0}{k_0} - \frac{1-k}{k}\sigma_1 - \frac{(1-k)^2}{k}\frac{\sigma_0}{k_0} - (1-k). \end{aligned}$$

Without losing generality, k_1 is taken as zero. For the nontrivial solution from Eqs.(68)–(71), the solvability condition is

$$\begin{aligned} \sigma_1 = \frac{1}{\lambda + k_0(1+\hat{k})S^{-1}\hat{M} + (1+\hat{k})\frac{1-k}{k}M_C} \times \Bigg\{ &-\Delta G_2 + \frac{g_{S1}}{1+\hat{k}}\left(\frac{\sigma_0}{k_0} - \Delta G_1\right) + \hat{k}g_1\left(\lambda\frac{\sigma_0}{k_0} + \hat{k}\Delta G_1\right) \\ &+ (1+\hat{k})k_0\left(\frac{1-k}{k}M_c - G_{S1}\right) + M_C(1+\hat{k})\left(q_1\frac{1-k}{k}\frac{\sigma_0}{k_0} - \frac{(1-k)^2}{k}\frac{\sigma_0}{k_0} - (1-k)\right)\Bigg\}. \end{aligned} \tag{72}$$

Consequently, we obtain the modified Mullins–Sekerka dispersion relation:[21]

$$\sigma \approx \sigma_0 + \varepsilon\sigma_1. \tag{73}$$

If $\sigma \sim \sigma_0 + \varepsilon^2\sigma_1 > 0$, the solidification system is unstable. If $\sigma \sim \sigma_0 + \varepsilon^2\sigma_1 < 0$, the solidification system is stable. The neutral stability curve is obtained for

$$\sigma \sim \sigma_0 + \varepsilon\sigma_1 \approx 0. \tag{74}$$

Figure 2 shows the dispersion relation (73) for different values of undercooling parameter. As the undercooling parameter increases, the range of morphological stability of the interface is decreased, and the critical wave number tends to increase. It is seen from Eq.(73) that the anisotropic surface energy is

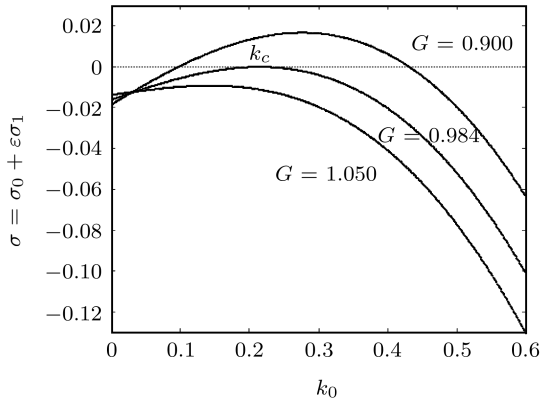


Fig.2. The dispersion relation (73) for different values of undercooling parameter $G_{L1} = G_{S1} = 0.900, 0.984, 1.050$, where $\alpha_4 = 0.0021$, $\lambda = 0.001$, $M_C = 0.125$, $S = 0.35$, $\hat{M} = 0.175$, $\varepsilon = 0.12$, $G_2 = 0$, $\hat{k} = 1.40, k = 0.103$.

always a destabilizing agent and the kinetic coefficient is always a stable factor. Figure 3 shows the dispersion relation (73) for different values of the anisotropic surface energy parameter. As the anisotropic surface energy parameter increases the critical wave number tends to increase.

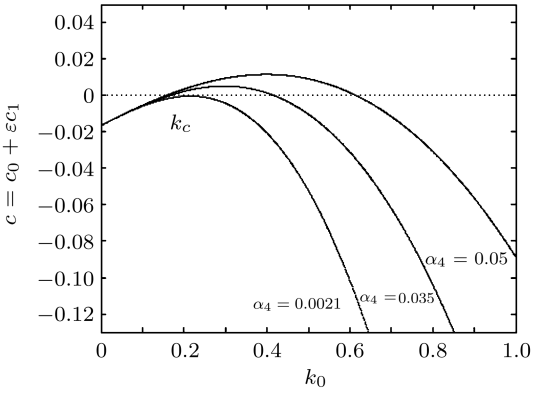


Fig.3. The dispersion relation (73) for different values of anisotropic surface energy parameter $\alpha_4 = 0.0021$, 0.035, 0.05, where $\lambda = 0.001$, $M_C = 0.125$, $S = 0.35$, $\hat{M} = 0.175$, $\varepsilon = 0.12$, $G_{L1} = G_{S1} = 0.984$, $G_2 = 0$, $\hat{k} = 1.40$, $k = 0.103$.

For the absolute stability analysis, we use the following notation:

$$\tilde{k} = \frac{k}{\varepsilon}, \qquad \tilde{\sigma}_0 = \frac{\sigma_0}{\varepsilon}. \tag{75}$$

We choose the capillary length ℓ_c to replace ℓ_D, we can use the dimensionless growth velocity $\hat{V} = \varepsilon^2 = \ell_c V/\kappa_D$ and concentration at the far field $\hat{C}_\infty = M_C(1-k)/k$, the dimensionless temperature gradient is taken as $\hat{G} = \hat{V}G$. Then the dispersion relation (73) is written as

$$\tilde{\sigma} = \tilde{\sigma}(\tilde{k}) = \tilde{\sigma}_0 + \varepsilon\tilde{\sigma}_1. \tag{76}$$

By setting

$$\tilde{\sigma}'(\tilde{k}) = 0, \tag{77}$$

we obtain the critical wave number

$$\tilde{k}_c = \sqrt[3]{-\frac{q}{2} + \sqrt{\left(\frac{q}{2}\right)^2 + \left(\frac{p}{3}\right)^3}} + \sqrt[3]{-\frac{q}{2} - \sqrt{\left(\frac{q}{2}\right)^2 + \left(\frac{p}{3}\right)^3}} - \frac{b}{3a}, \tag{78}$$

where

$$p = \frac{c}{a} - \frac{b^2}{3a^2}, \qquad q = \frac{2b^3}{27a^3} - \frac{cb}{3a^2} + \frac{d}{a}, \quad a = 4Q_1^2Q_2(1-15\alpha_4)^2\hat{V}^2, \quad b = -3(1+\hat{k})(1-15\alpha_4)\hat{V},$$
$$c = \left(4Q_1^2Q_2\left(\frac{\hat{G}}{\hat{V}} - \hat{C}_\infty\right) + 2Q_1\Pi_1\right)(1-15\alpha_4)\hat{V}, \quad d = (1+\hat{k})\left(\sqrt{\hat{V}}\left(\hat{C}_\infty - \frac{\hat{G}_{S1}}{\hat{V}}\right) - \frac{\hat{G}}{\hat{V}} + \hat{C}_\infty\right),$$

$$\Pi_1 = \left(\frac{\lambda\alpha_T}{2} - \frac{\lambda(1+\hat{k})\hat{k}^2}{2}\right)\frac{\Delta\hat{G}_1}{\hat{V}} + (1+\hat{k}^2)\left(\frac{1}{2} - k\right)\hat{C}_\infty + \frac{\lambda\alpha_T}{2} - \frac{\lambda^2(1+\hat{k})\hat{k}}{2},$$

$$Q_1 = \frac{1}{\lambda + (1+\hat{k})\hat{C}_\infty}, \quad Q_2 = (1+\hat{k})\left(\frac{(1+\hat{k})^2}{2}\hat{C}_\infty + \frac{\lambda\alpha_T}{2} + \frac{\lambda^2(1+\hat{k})\hat{k}}{2}\right).$$

From

$$\tilde{\sigma}(\tilde{k}) = 0, \tag{79}$$

we obtain the absolute stability criterion

$$Q_1^2Q_2\left((1-15\alpha_4)\hat{V}\tilde{k}_c^2 + \frac{\hat{G}}{\hat{V}} - \hat{C}_\infty\right)^2 + Q_1\Pi_1\left((1-15\alpha_4)\hat{V}\tilde{k}_c^2 + \frac{\hat{G}}{\hat{V}} - \hat{C}_\infty\right)$$
$$+\left(\sqrt{\hat{V}}\left(\hat{C}_\infty - \frac{\hat{G}_{S1}}{\hat{V}}\right) - (1-15\alpha_4)\hat{V}\tilde{k}_c^2 - \frac{\hat{G}}{\hat{V}} + \hat{C}_\infty\right)(1+\hat{k})\tilde{k}_c + \Pi_3 = 0, \tag{80}$$

where

$$\Pi_3 = -\frac{\Delta\hat{G}_2}{\hat{V}} + \left(\frac{\lambda\alpha_T}{2(1+\hat{k})} + \frac{\lambda\hat{k}^2}{2}\right)\frac{\Delta\hat{G}_1}{\hat{V}} - (1+\hat{k})k\hat{C}_\infty.$$

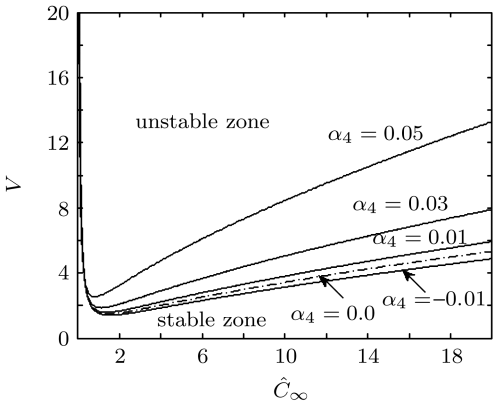


Fig.4. The range of the modified Mullins–Sekerka absolute stability in the ($\hat{C}_\infty$, $\hat{V}$) plain for different values of the anisotropic surface energy parameter α_4: $\alpha_4 = -0.01$, 0.00, 0.01, 0.03, 0.05, where $\lambda = 0.001$, $M_C = 0.125$, $S = 0.35$, $\varepsilon = 0.12$, $G_{L1} = G_{S1} = 0.984$, $G_2 = 0$, $\hat{G} = 0.01$, $\hat{k} = 1.40$, $k = 0.103$.

4. Conclusions

By using the multi-variable expansion method developed by Xu,[13−20] we have made a more careful analysis for the effect of the anisotropic surface tension on the directional solidification. When the expression exhibiting the four-fold symmetry is included, the linear stability analysis demonstrates an analogous analysis without the anisotropic surface tension made by Xu in Refs.[13, 14]. For the moderate wave number $k_0 = O(1)$, we obtain the uniformly valid asymptotic solution for the solidification system and the absolute stability criterion is obtained. Our linear stability analysis reveals that for the given temperature gradient, as the anisotropic surface tension parameter increases, the stability zone tends to decrease.

It should be pointed out that for the small wave number $k_0 \gg O(1/\varepsilon)$, our resulting asymptotic solution is not uniformly valid, it is needed to consider the effect of the anisotropic surface tension on the directional solidification in the extremely short-wave region in another paper.

References

[1] William R W 1970 *J. Crystal Growth* **7** 203

[2] Coriell S R and Sekerka R F 1976 *J. Crystal Growth* **34** 157

[3] Young G W, Davis S H and Brattkus K 1987 *J. Crystal Growth* **83** 560

[4] Vigdergauz S and Givoli D 1999 *J. Crystal Growth* **198-199** 125

[5] Satoa M and Uwahaa M 1999 *J. Crystal Growth* **198-199** 38

[6] Golovin A A and Davis S H 1998 *Physica* D **116** 363

[7] Coriell S R and McFadden G B 2002 *J. Crystal Growth* **237-239** 8

[8] Guo Weidong and Johnson D T 2004 *J. Crystal Growth* **268** 258

[9] Norris S A, Davis S H, Watson S J and Voorhees P W 2008 *J. Crystal Growth* **310** 414

[10] Davis S H 2001 *Theory of Solidification* (Cambridge: Cambridge University Press)

[11] Lü H L, Zhang Y M and Zhang Y M 2003 *Chin. Phys.* **12** 895

[12] Yan Y, Xu S W, Jin H M, Du X B and Su F 2004 *Chin. Phys.* **13** 1965

[13] Xu J J 2006 *Introduction to Kinetics of Solidification and Stability Theory of the Interface* (Beijing: Science Press)

[14] Xu J J 1998 *Interfacial Wave Theory of Pattern Formation: Selection of Dendritic Growth and Viscous Fingering in Hele–Shaw Flow* (New York: Springer)

[15] Xu J J 1991 *Euro. J. Appl. Math.* **2** 105

[16] Xu J J 1993 *J. Crystal Growth* **128** 219

[17] Xu J J 1994 *J. Fluid Mech.* **263** 227

[18] Xu J J 1996 *Euro. J. Appl. Math.* **7** 169

[19] Xu J J 1996 *Phys. Rev.* E **53** 5051

[20] Xu J J 2006 *J. Crystal Growth* **292** 523

[21] Mullins W W and Sekerka R F 1964 *J. Appl. Phys.* **35** 444